Supplemental Materials

Molecular Biology of the Cell

Emmerstorfer-Augustin et al.

SUPPLEMENTAL MATERIAL

Tracking yeast pheromone receptor Ste2 endocytosis

using fluorogen-activating protein (FAP) tagging

Anita Emmerstorfer-Augustin, Christoph M. Augustin, Shadi Shams, Jeremy Thorner

Table of Contents:

Evaluation of diverse leader sequences to ensure maximal functional expression, proper plasma membrane delivery, and optimal fluorescence of FAP-Ste2 constructs

To optimize expression, folding, membrane insertion, and capacity for fluorogen labeling of the FAPα2-Ste2-FLAG-$(His)_6$ chimera, a variety of different signal sequences, alone and in combination, were tested (Fig. S2A; Table S1), including: the signal sequence of human immunoglobin *kappa* light chain (Igκ) (Szent-Gyorgyi *et al.*, 2008); the prepro-leader segment of one of the precursors (MFα1) from which yeast α-factor pheromone is generated (Flessel *et al.*, 1989); the endogenous N-terminal secretion signal of Ste2 itself (Konopka & Thorner, 2013); and, the signal sequence of the secreted isoform of yeast invertase (Suc2) (Carlson *et al.*, 1983). We took special interest in the prepro-leader of MFα1 because it has been used successfully to direct efficient secretion of many other proteins from yeast cells (Emr *et al.*, 1983; Brake, *et al.*, 1984; Zsebo *et al.*, 1986). Synthesis and export of mature bioactive α-factor (13 residues) occurs in the yeast secretory pathway of *MAT*α cells (Julius *et al.*, 1984b). Production of the pheromone requires processing of prepro-α-factor (165 residues) and excision

of the four copies of α-factor embedded in this precursor by four proteases: signal peptidase (Waters *et al.*, 1988); endoprotease Kex2 (Julius *et al.*, 1984a); dipeptidyl aminopeptidase Ste13 (Julius *et al.*, 1983); and, carboxypeptidase B Kex1 (Dmochowska *et al.*, 1987). After import into the secretory pathway, signal (pre-) sequence removal, and N-linked glycosylation of the pro-segment, Kex2, which is highly specific for cleaving on the carboxyl side of -KR- sites situated upstream of each α-factor repeat (Rockwell & Thorner, 2004), is essential for initiating the maturation process, and thereby removes the pro-segment (Julius *et al.*, 1984a). For secretion of heterologous proteins mediated by the prepro-leader of MFα1, several studies have demonstrated that Kex2 cleavage is important for efficient secretion (Brake et al., 1984, Yang *et al.*, 2013; Fitzgerald & Glick, 2014). Hence, in constructs containing the MFα1 prepro-leader, we tested versions that either lacked ($MF\alpha1^{1-83}$) or carried ($MF\alpha1^{1-87}$) the most upstream Kex2 cleavage site (Fig. S2A). The rationale for generating hybrid constructs that included either the original (Igκ) or a truncated version ($Ig\kappa^{1-10}$) of the Igκ signal sequence from the FAPα2 tag itself was to assess whether it might be important for the stability and/or folding of the rest of this immunoglobulin-derived fluorogen-activating protein. Likewise, the reasoning behind testing the N-terminal sequence of Ste2 itself (Ste^{1-51}) was to ascertain whether native N-glycosylation, which normally occurs at two Asn residues within this region, might be important for efficient secretion of our FAPα2-Ste2 fusion protein, even though mutational analysis indicates that N-glycosylation is unnecessary for proper translocation of Ste2 itself to the plasma membrane (Mentesana & Konopka, 2001). On the other hand, and not surprislngly, it has been shown that a large deletion (residues 11-30) within this N-terminus segment of Ste2 abrogates delivery of the receptor to the plasma membrane (Uddin *et al.*, 2015). The reason we also examined the efficacy of the signal sequence (residues 1-19) of Suc2 is that it has also been used successfully to direct secretion of a number of heterologous proteins from yeast cells (Chang et al., 1986, Driedonks *et al.*, 1995, Hashimoto *et al.*, 1998).

To ensure that every cell had the capacity to express the variant of interest, and did so from the endogenous *STE2* promoter, each of these constructs was integrated, as follows, into the genome at the *STE2* locus on chromosome VI in *MAT**a*** strain JTY4470 (Table 1), a derivative of BY4741 containing a *ste2*Δ::KanMX allele. For integration of the Igκ-FAPα2-Ste2-FLAG-$(His)_6$ cassette, which includes the *CYC1* transcription terminator ($CYC1_{tt}$) and *URA3* as the selectable marker, into the *STE2* locus by homologous recombination, we used a PCR-based approach (Longtine *et al.*, 1998). The Igκ-FAPα2-Ste2-FLAG-$(His)_6$ sequence in *CEN* plasmid pAEA30 [pRS416-$STE2_{prom}$(560 bp)-Igκ-FAPα2-Ste2-FLAG-$(His)_6$-$CYC1_{tt}$(364 bp)-*URA3*] was amplified by PCR using a forward primer corresponding to the Igκ leader sequence (including its ATG start codon), which also included at its 5'-end 40 nucleotides homologous to the sequence upstream of the ATG start codon of the *STE2* locus, and a reverse primer corresponding to the sequence downstream of the *URA3* marker, which also included 40 nucleotides homologous to the sequence downstream of the TAA stop codon of the *STE2* ORF. The resulting PCR product was used for DNA-mediated transformation (Amberg *et al.*, 2006), selecting for Ura^+ transformants and scoring them for concomitant loss of kanamycin (G418) resistance. To remove the Igκ signal sequence and substitute alternative leader sequences, or to combine the Igκ signal sequence with different leader sequences, we spliced the relevant sequences together using the PCR method known as overlap extension (Horton et al., 1993). In brief, DNA fragments containing the desired leader sequences and containing appropriate complementary ends to permit their annealing to each other and to the FAPα2-Ste2 cassette were amplified by PCR; these fragments were annealed to each other and to either Igκ-FAPα2-Ste2-FLAG-$(His)_6$ or FAPα2-Ste2-FLAG-$(His)_6$ DNA and then extended in a second round of PCR using the same forward and reverse primers described above. The resulting PCR products were used to transform the *MAT***a** cells. Correct assembly and proper integration of each construct was confirmed by colony PCR and direct sequencing of the DNA spanning the entire *STE2* locus.

The level of expression of each FAPα2-Ste2 variant was assessed by immunoblot analysis

(Fig. S2B), as described in Materials and Methods. Depending on the length and composition of its respective leader sequence and in the absence of any posttranslational modification, the FAPα2-Ste2 variants should have molecular masses of 89-92 kDa; however, all of the FAPα2-Ste2 constructs that contained any combination of MFα1 or *STE2*$^{(1-51)}$ were N-glycosylated, yielding species with molecular masses of ~120 kDa. The weakest expression was observed for the Igκ leader alone and for the composite *STE2*$^{(1-51)}$-Igκ leader (Fig. S2B, lanes 1 and 8). All of the other constructs yielded a level of expressed protein quite comparable to the otherwise native Ste2-FLAG-$(His)_6$ control (Fig. S2B, left side). For variants harboring the Kex2 cleavage site, the ~120 kDa species was processed to the size expected for FAPα2-Ste2 (~95 kDa) (Fig. S2B, lanes 2, 4 and 7). However, we also noted that for all of the constructs, except those with the Suc2 leader (Fig. S2B, lanes 10 and 11), a species was present equivalent in size to the Ste2-FLAG-$(His)_6$ control, which indicated that non-specific proteolysis was cleaving the FAPα2 domain off of these chimeras. The source of this cleavage and how this problem was surmounted in described in the main text.

Aside from a near-native level of expression, the next most important criterion to assess to settle on the most desirable construct was whether the receptor portion of each construct was properly folded and functional. For this reason, the ability of cells expressing each construct to respond to α-factor was examined using a standard agar diffusion bioassay that measures mating pheromone-induced growth arrest (Reneke et al., 1988). Strikingly, only those chimeras that were not proteolyzed to a size corresponding to Ste2-FLAG-$(His)_6$ yielded a distinctly weaker (Fig. S2B, lane 10) or much weaker (Fig. S2B, lanes 1 and 11) response than all of the other constructs or the control cells expressing Ste2-FLAG-$(His)_6$ (Fig. S2C). Hence, even though the FAPα2-Ste2 chimera generated using the composite Suc2(1-19)-Igκ was full-length and yielded a readily detectable pheromone response, we were concerned that this assay might not accurately reflect the properties of the intact FAPα2-Ste2 chimera, but might be confounded

by how readily each construct was converted to a form that had lost its FAPα2 tag. However, as demonstrated in the main text, when completely intact, the FAPα2-Ste2 chimera generated using the composite MFα1(1-83)-Igκ leader, which we used in the bulk of our work, yields a response to pheromone equivalent to that of control cells expressing Ste2-FLAG-$(His)_6$ (see Fig. 3D).

Finally, to choose the most desirable construct for our purposes, we also had to assess the folding and function of the FAP2α portion of each chimera, a criterion just as important as the expression level and receptor competence of each construct. Toward that end, cells expressing each of the constructs were incubated with fluorogen, as described in detail in Materials and Methods, and the pixel intensities of 200-300 cells per strain were quantified (Fig. S2D) using CellProfiler (see modified CellProfiler code provided in the accompanying cell_analysis.cppipe file). The FAPα2-Ste2 chimera generated using the Igκ leader alone yielded readily detectable, but rather dim fluorescence (Fig. S2D, lane 1; see also Fig. S1C). This property cannot be attributed to its low level of expression because the FAPα2-Ste2 chimera generated using the composite Ste2(1-51)-Igκ leader was also poorly expressed, but yielded distinctly brighter fluorescence (Fig. S2D). Conversely, despite their very robust expression (Fig. S2B), the FAPα2-Ste2 chimeras generated using the composite Suc*2*(1-19)-Igκ leader or the Suc2(1-19) signal sequence alone yielded very poor fluorescent signals (Fig. S2D), indicating misfolding of the FAP2α tag in these constructs. Reproducibly, however, the FAPα2-Ste2 chimera generated using the composite MFα1(1-83)-Igκ leader exhibited the brightest fluorescent signal. Interestingly, its nearly identical sister construct in which the MFα1 sequence used included the Kex2 cleavage site, the fluorescent signal was routinely reduced by at least 50% (Fig. S2D).

Based on expression level, receptor functionality, and fluorogen activation, we selected the MFα1(1-83)-Igκ-FAPα2-Ste2-FLAG-$(His)_6$ chimera for the majority of the experiments described in this study.

Access to Custom CellProfiler Pipeline

CellProfiler is free, open-source software for measuring and analyzing digital images (Carpenter AE et al., 2006; Kamentsky L et al., 2011) [see also: http://cellprofiler.org]. The CellProfiler software needs instructions about how to handle the features in the images of interest; the developers of CellProfiler refer to that set of instructions as a "pipeline" and the corresponding ASCII code containing those instructions is designated a .cppipe file. The file ending must be .cppipe because the .cppipe appendage / descriptor is how the CellProfiler program recognizes it as the specific pipeline to use.

For the purposes described in this paper, we developed a customized .cppipe to process and analyze the features of interest to us (plasma membrane, endosomes, vacuolar membrane, vacuole contents) in images of yeast cells captured by fluorescence microscopy. So that this resource is readily available to any other investigator, upon final acceptance of this manuscript for publication, we will provide our .cppipe itself (or in .zip file format) to any researcher free-of-charge upon request.

Literature Cited

Amberg DC, Burke DJ, Strathern JN (2006) High-efficiency transformation of yeast. *CSH Protoc*. doi: 10.1101/pdb.prot4145.

Brake AJ, Merryweather JP, Coit DG, Heberlein UA, Masiarz FR, Mullenbach GT, Urdea MS, Valenzuela P, Barr PJ (1984) Alpha-factor-directed synthesis and secretion of mature foreign proteins in *Saccharomyces cerevisiae*. *Proc. Natl. Acad. Sci. USA* **81**: 4642-4646.

Carlson M, Taussig R, Kustu S, Botstein D (1983) The secreted form of invertase in Saccharomyces cerevisiae is synthesized from mRNA encoding a signal sequence. *Mol. Cell. Biol.* **3**: 439-447.

Carpenter AE, Jones TR, Lamprecht MR, Clarke C, Kang IH, Friman O, Guertin DA, Chang JH, Lindquist RA, Moffat J, Golland P, Sabatini DM (2006) CellProfiler: image analysis software for identifying and quantifying cell phenotypes. *Genome Biology* **7**: R100.

Chang CN, Matteucci M, Perry LJ, Wulf JJ, Chen CY, Hitzeman RA (1986) *Saccharomyces cerevisiae* secretes and correctly processes human interferon hybrid proteins containing yeast invertase signal peptides. *Mol Cell Biol* **6**: 1812-1819.

Dmochowska A, Dignard D, Henning D, Thomas DY, Bussey H (1987) Yeast *KEX1* gene encodes a putative protease with a carboxypeptidase B-like function involved in killer toxin and alpha-factor precursor processing. *Cell* **50**: 573-584.

Driedonks RA, Toschka HY, van Almkerk JW, Schäffers IM, Verbakel JM (1995) Expression and secretion of antifreeze peptides in the yeast *Saccharomyces cerevisiae*. *Yeast* **11**: 849-864.

Emr SD, Schekman R, Flessel MC, Thorner J (1983) An *MFα1-SUC2* (prepro-α-factor-invertase) gene fusion for study of protein localization and gene expression in yeast. *Proc. Natl. Acad. Sci. USA* **80**: 7080-7084.

Fitzgerald I, Glick BS (2014) Secretion of a foreign protein from budding yeasts is enhanced by cotranslational translocation and by suppression of vacuolar targeting. *Microb. Cell Fact*. **13**: 125.1-125.12.

Flessel MC, Brake AJ, Thorner J (1989) The *MFα1* gene of *Saccharomyces cerevisiae*: genetic mapping and mutational analysis of promoter elements. *Genetics* **121**: 223-236.

Hashimoto Y, Koyabu N, Imoto T (1998) Effects of signal sequences on the secretion of hen lysozyme by yeast: construction of four secretion cassette vectors. *Protein. Eng.* **11**: 75-77.
Horton RM, Ho SN, Pullen JK, Hunt HD, Cai Z, Pease LR (1993) Gene splicing by overlap extension. *Methods Enzymol.* **217**: 270-279.

Julius D, Blair L, Brake A, Sprague G, Thorner J (1983) Yeast α-factor is processed from a larger precursor polypeptide: the essential role of a membrane-bound dipeptidyl aminopeptidase. *Cell* **32**: 839-852.

Julius D, Brake A, Blair L, Kunisawa R, Thorner J (1984a) Isolation of the putative structural gene for the lysine-arginine-cleaving endopeptidase required for processing of yeast prepro-alpha-factor. *Cell* **37**: 1075-1089.

Julius D, Schekman R, Thorner J (1984b) Glycosylation and processing of prepro-α-factor through the yeast secretory pathway. *Cell* **36**: 309-318.

Kamentsky L, Jones TR, Fraser A, Bray M, Logan D, Madden K, Ljosa V, Rueden C, Harris GB, Eliceiri K, Carpenter AE (2011) Improved structure, function, and compatibility for CellProfiler: modular high-throughput image analysis software. *Bioinformatics* **27**: 1179-1180.

Konopka JB, Thorner JW (2013) Pheromone Receptors (Yeast). In: Lennarz WJ, Lane MD (eds.) The Encyclopedia of Biological Chemistry, 2nd Edition, Waltham, MA: Academic Press, Inc., Vol. 3, pp. 441-446.

Longtine MS, McKenzie A 3rd, Demarini DJ, Shah NG, Wach A, Brachat A, Philippsen P, Pringle JR (1998) Additional modules for versatile and economical PCR-based gene deletion and modification in Saccharomyces cerevisiae. *Yeast* **14**: 953-961.

Mentesana PE, Konopka JB (2001) Mutational analysis of the role of N-glycosylation in α-factor receptor function. *Biochemistry* **40**: 9685-9694.

Reneke JE, Blumer KJ, Courchesne WE, Thorner J (1988) The carboxy-terminal segment of the yeast α-factor receptor is a regulatory domain. *Cell* **55**: 221-234.

Rockwell NC, Thorner JW (2004) The kindest cuts of all: crystal structures of Kex2 and furin reveal secrets of precursor processing. *Trends Biochem Sci*. **29**: 80-87.

Schindelin J, Arganda-Carreras I, Frise E, Kaynig V, Longair M, Pietzsch T, Preibisch S, Rueden C, Saalfeld S, Schmid B, Tinevez JY, White DJ, Hartenstein V, Eliceiri K, Tomancak P, Cardona A (2012) Fiji: an open-source platform for biological-image analysis. *Nat. Methods* **9**: 676-682.

Szent-Gyorgyi C, Schmidt BF, Creeger Y, Fisher GW, Zakel KL, Adler S, Fitzpatrick JA, Woolford CA, Yan Q, Vasilev KV, Berget PB, Bruchez MP, Jarvik JW, Waggoner A (2008) Fluorogen-activating single-chain antibodies for imaging cell surface proteins. *Nat. Biotechnol.* **26**: 235-240.

Uddin MS, Hauser M, Naider F, Becker JM (2015) The N-terminus of the yeast G protein-coupled receptor Ste2p plays critical roles in surface expression, signaling, and negative regulation. *Biochim. Biophys. Acta* **1858**: 715-724.

Waters MG, Evans EA, Blobel G (1988) Prepro-α-factor has a cleavable signal sequence. *J. Biol. Chem.* **263**: 6209-6214.

Yang H, Rudge DG, Koos JD, Vaidialingam B, Yang HJ, Pavletich NP (2013) mTOR kinase structure, mechanism and regulation. *Nature* **497**: 217-223.

Zsebo KM, Lu HS, Fieschko JC, Goldstein L, Davis J, Duker K, Suggs SV, Lai PH, Bitter GA (1986) Protein secretion from *Saccharomyces cerevisiae* directed by the prepro-α-factor leader region. *J. Biol. Chem*. **261**: 5858-5865.

SUPPLEMENTAL TABLES

Table S1. Yeast strains used for testing different signal sequences.

yAEA144	BY4741 *STE2*$_{prom}$-Igκ-FAPα2-*STE2*-FLAG-(His)$_6$::*URA3*	This study
yAEA143	BY4741 *STE2*$_{prom}$-Igκ-FAPβ1-Ste2-FLAG-(His)$_6$::URA3	This study
yAEA145	BY4741 *STE2*$_{prom}$-MFα1$_{(1-87)}$-FAPα2-*STE2*-FLAG -(His)$_6$::*URA3*	This study
yAEA152	BY4741 *STE2*$_{prom}$-MFα1$_{(1-83)}$-Igκ-FAPα2-*STE2*-FLAG -(His)$_6$::*URA3* [**FAP-Ste2**]	This study
yAEA153	BY4741 *STE2*$_{prom}$-MFα1$_{(1-87)}$-Igκ-FAPα2-*STE2*-FLAG -(His)$_6$::*URA3*	This study
yAEA169	BY4741 *STE2*$_{prom}$-MFα1$_{(1-83)}$-FAPα2-*STE2*-FLAG-(His)$_6$::*URA3*	This study
yAEA170	BY4741 *STE2*$_{prom}$-MFα1$_{(1-83)}$-Igκ$_{(1-10)}$-FAPα2-*STE2*-FLAG-(His)$_6$::*URA3*	This study
yAEA171	BY4741 *STE2*$_{prom}$-MFα1$_{(1-87)}$-Igκ$_{(1-10)}$-FAPα2-*STE2*-FLAG-(His)$_6$::*URA3*	This study
yAEA172	BY4741 *STE2*$_{prom}$-Ste2$_{(1-51)}$-Igκ-FAPα2-*STE2*-FLAG-(His)$_6$::*URA3*	This study
yAEA173	BY4741 *STE2*$_{prom}$-Ste2$_{(1-51)}$-FAPα2-*STE2*-FLAG-(His)$_6$::*URA3*	This study
yAEA205	BY4741 *STE2*$_{prom}$-Suc2$_{(1-19)}$-Igκ-FAPα2-*STE2*-FLAG-(His)$_6$::*URA3*	This study
yAEA206	BY4741 *STE2*$_{prom}$-Suc2$_{(1-19)}$-FAPα2-*STE2*-FLAG -(His)$_6$::*URA3*	This study
yAEA256	BY4741 *ste2Δ::STE2*$_{prom}$-FAP-STE2 *sst2Δ*::Hyg	This study

Table S2. Nucleotide sequence of MFα1$_{(1-83)}$-Igκ-FAPα2-*STE2* [abbreviated FAP-Ste2].

Underlined, MFα1$_{(1-83)}$ prepro-leader; **bold**, Igκ signal sequence; blue, HA-tag; magenta, FAPα2; green, myc-tag; *italics*, full-length *STE2*; red, FLAG tag; orange, (His)$_6$-tag.

ATGAGATTTCCTTCAATTTTTACTGCAGTTTTATTCGCAGCATCCTCCGCATTAGCTGCTCCAGTCAACACTACAACA
GAAGATGAAACGGCACAAATTCCGGCTGAAGCTGTCATCGGTTACTTAGATTTAGAAGGGGATTTCGATGTTGCT
GTTTTGCCATTTTCCAACAGCACAAATAACGGGTTATTGTTTATAAATACTACTATTGCCAGCATTGCTGCTAAAGA
AGAAGGGGTATCTTTGGAT**ATGGAGACAGACACACTCCTGCTATGGGTACTGCTGCTCTGGGTTCCAGGTTCCAC**
TGGTGACTATCCATATGATGTTCCAGATTATGCTGGGGCCCAGCCGGCCCAGGCCGTCGTTACCCAAGAACCTAGT
GTTACCGTTAGCCCAGGTGGTACTGTTATACTTACTTGTGGAAGTGGTACGGGTGCCGTCACATCTGGTCATTATG
CAAATTGGTTTCAACAAAAACCAGGACAAGCTCCAAGAGCTTTGATTTTTGATACTGATAAGAAGTATTCTTGGAC
CCCAGGTAGATTTTCTGGATCTTTGCTGGGAGCAAAGGCAGCTTTGACAATATCAGATGCTCAGCCTGAGGACGA
AGCCGAGTATTACTGTTCTCTTAGCGACGTGGATGGCTACTTGTTTGGCGGTGGAACACAACTGACGGTTCTGTCC
GGTGGTGGCGGCTCTGGTGGCGGTGGCAGCGGCGGTGGTGGTTCCGGAGGCGGCGGTTCTCAGGCTGTGGTGA
CTCAGGAGCCGTCAGTGACTGTGTCCCCAGGAGGGACAGTCATTCTCACTTGTGGCTCCGGCACTGGAGCTGTCA
CCAGTGGTCATTATGCCAACTGGTTCCAGCAGAAGCCTGGCCAAGCCCCCAGGGCACTTATATTTGACACCGACAA
GAAGTATTCCTGGACCCCTGGCCGATTCTCAGGCTCCCTCCTTGGGGCCAAGGCTGCCCTGACCATCTCGGATGCG
CAGCCTGAAGATGAGGCTGAGTATTACTGTTCGCTCTCCGACGTTGACGGTTATCTGTTCGGAGGAGGCACCCAG
CTGACCGTCCTCTCCGGCCGCAGGGGCCGGGATCCGCGGCTGCAGGTCGACGAACAAAAACTCATCTCAGAAGA
GGATCTG*ATGTCTGATGCGGCTCCTTCATTGAGCAATCTATTTTATGATCCAACGTATAATCCTGGTCAAAGCACCA*
TTAACTACACTTCCATATATGGGAATGGATCTACCATCACTTTCGATGAGTTGCAAGGTTTAGTTAACAGTACTGTT
ACTCAGGCCATTATGTTTGGTGTCAGATGTGGTGCAGCTGCTTTGACTTTGATTGTCATGTGGATGACATCGAGAA
GCAGAAAAACGCCGATTTTCATTATCAACCAAGTTTCATTGTTTTTAATCATTTTGCATTCTGCACTCTATTTTAAATA
TTTACTGTCTAATTACTCTTCAGTGACTTACGCTCTCACCGGATTTCCTCAGTTCATCAGTAGAGGTGACGTTCATGT
TTATGGTGCTACAAATATAATTCAAGTCCTTCTTGTGGCTTCTATTGAGACTTCACTGGTGTTTCAGATAAAAGTTAT
TTTCACAGGCGACAACTTCAAAAGGATAGGTTTGATGCTGACGTCGATATCTTTCACTTTAGGGATTGCTACAGTTA
CCATGTATTTTGTAAGCGCTGTTAAAGGTATGATTGTGACTTATAATGATGTTAGTGCCACCCAAGATAAATACTTC
AATGCATCCACAATTTTACTTGCATCCTCAATAAACTTTATGTCATTTGTCCTGGTAGTTAAATTGATTTTAGCTATTA
GATCAAGAAGATTCCTTGGTCTCAAGCAGTTCGATAGTTTCCATATTTTACTCATAATGTCATGTCAATCTTTGTTGG
TTCCATCGATAATATTCATCCTCGCATACAGTTTGAAACCAAACCAGGGAACAGATGTCTTGACTACTGTTGCAACA
TTACTTGCTGTATTGTCTTTACCATTATCATCAATGTGGGCCACGGCTGCTAATAATGCATCCAAAACAAACACAATT
ACTTCAGACTTTACAACATCCACAGATAGGTTTTATCCAGGCACGCTGTCTAGCTTTCAAACTGATAGTATCAACAA
CGATGCTAAAAGCAGTCTCAGAAGTAGATTATATGACCTATATCCTAGAAGGAAGGAAACAACATCGGATAAACA
TTCGGAAAGAACTTTTGTTTCTGAGACTGCAGATGATATAGAGAAAAATCAGTTTTATCAGTTGCCCACACCTACGA
GTTCAAAAAATACTAGGATAGGACCGTTTGCTGATGCAAGTTACAAAGAGGGAGAAGTTGAACCCGTCGACATGT
*ACACTCCCGATACGGCAGCTGATGAGGAAGCCAGAAAGTTCTGGACTGAAGATAATAATAATTTA*GACTACAAGG
ACGACGATGACAAGACCGGTGTGCCGCGCGGCAGCGGCAGCAGCCATCATCATCATCATCATAGCAGCGGCTAA

Table S3. Plasmids used in Fig. S1

Plasmid	Genotype	Reference or source
pRS416	*CEN URA3*	(Sikorski & Hieter, 1989)
pAEA66	pRS416-$STE2_{prom}$-*STE2*-FLAG-$(His)_6$	This study
pAEA30	pRS416-$STE2_{prom}$-Igk-FAPα2-Ste2-FLAG-$(His)_6$	This study
pAEA31	pRS416-$STE2_{prom}$-Igk-FAPβ1-Ste2-FLAG-$(His)_6$	This study

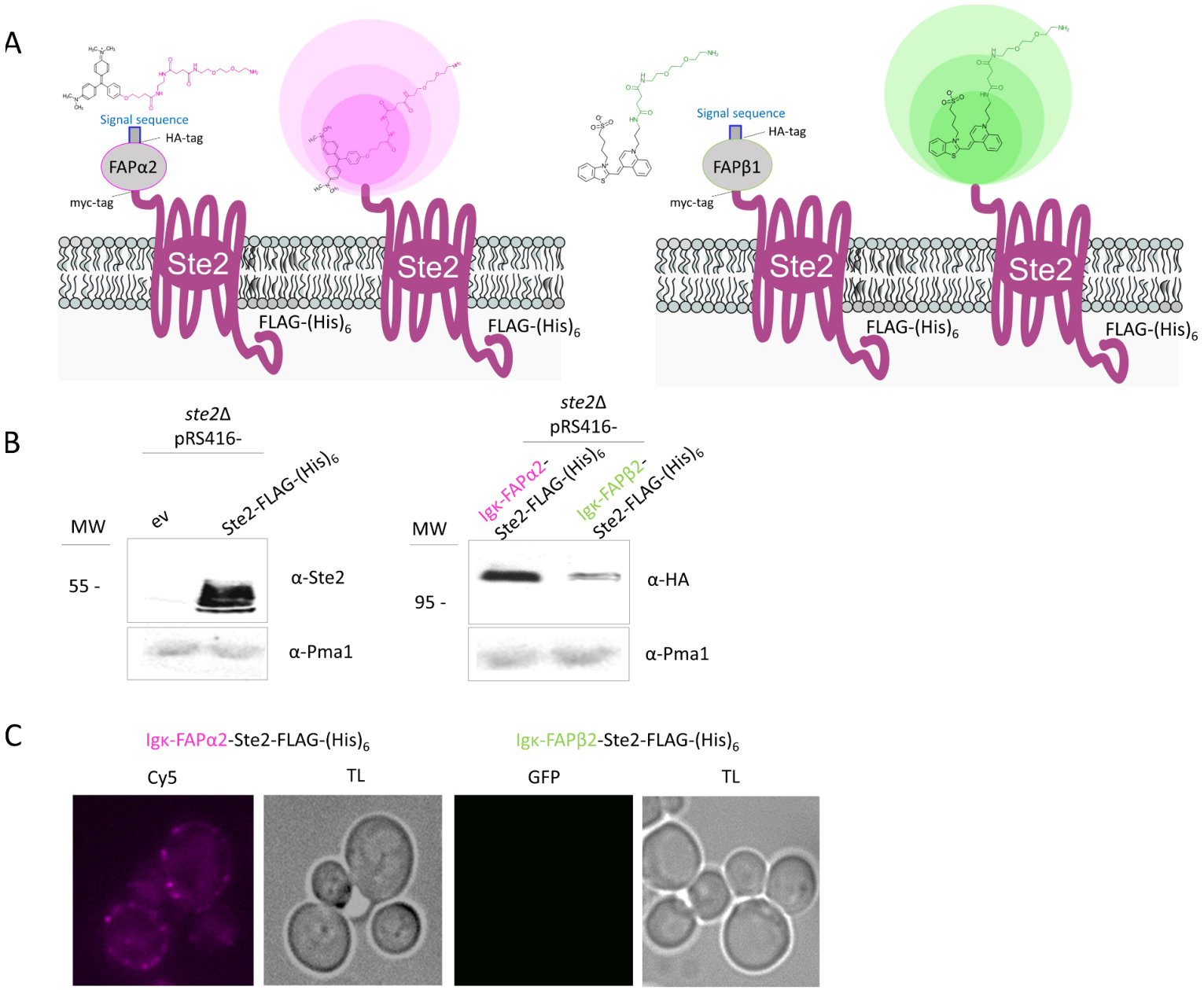

Fig. S1. N-terminal tagging of Ste2-FLAG-(His)$_6$ with Igκ-FAPα2 and Igκ-FAPβ1. (A) Extracellular tagging of Ste2 allows only receptors located at the plasma membrane to be visualized upon treatment with fluorogen; Igκ-FAPα2 and Igκ-FAPβ1 have been selectively engineered to become fluorescent upon binding of membrane-impermeable fluorogens, malachite green and thiazole orange derivatives, respectively. (B) Cells expressing either Ste2-FLAG-(His)$_6$ (yAEA201), Igk-FAPα2-Ste2-FLAG-(His)$_6$ (yAEA144), or Igk-FAPβ1-Ste2-FLAG-(His)$_6$ (yAEA143) from the endogenous *STE2* promoter on *CEN* plasmids (Table S3) were grown to early-exponential phase at 20˚C, membrane protein extracts prepared, resolved on an SDS-PAGE and analyzed by immunoblotting. (C) Cells expressing FAP-tagged Ste2 were incubated with the respective fluorogen at 30˚C for 15 min and imaged by fluorescence microscopy.

FIG. S2

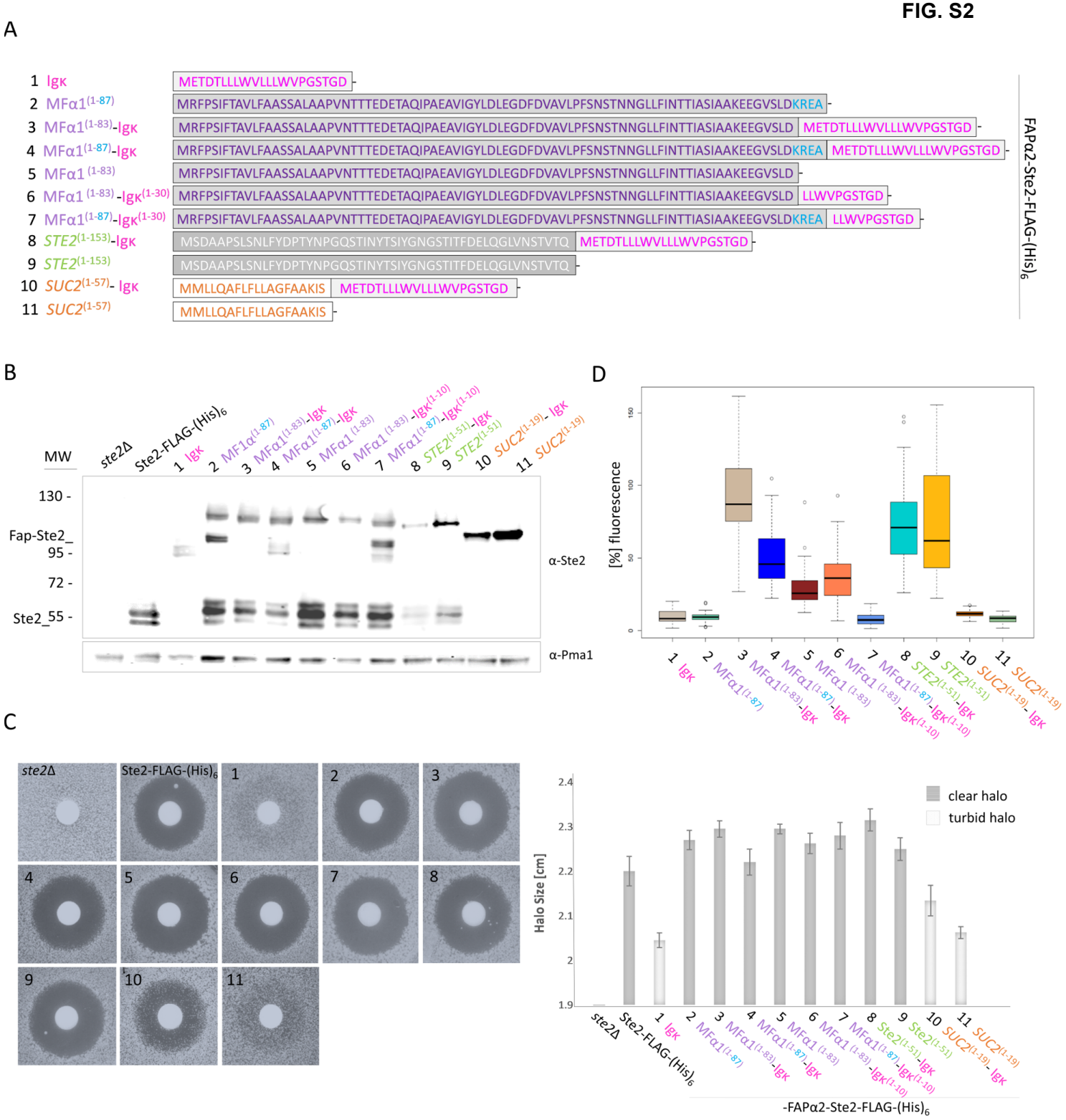

Fig. S2. Effect of endogenous yeast secretory signals on expression level, receptor function, and fluorescence intensity of FAPα2-Ste2. (A) The FAPα2 tag includes at its N terminus the leader peptide of a mammalian IgG *kappa* light chain (Igκ) as the secretion signal. The prepro-leader sequence of the α-factor precursor (MFα1), without (residues 1-83) or with (residues 1-

87) its Kex2 cleavage site, the N-terminal leader of Ste2 (residues 1-153), or the N-terminal signal peptide-containing sequence (residues 1-57) of secreted yeast invertase (Suc2) were inserted upstream of, or in place of, the Igκ sequence in FAPα2-Ste2, as indicated. (B) *MAT***a** *ste2*Δ strain (JTY4470) or derivatives expressing either *STE2*-Flag-$(His)_6$ (yAEA201) or each of the eleven constructs shown in (A), Igκ-FAPα2-*STE2* (yAEA144), $Mfα1_{(1-87)}$-FAPα2-*STE2* (yAEA145), $Mfα1_{(1-83)}$-Igκ-FAPα2-*STE2* (yAEA152), $Mfα1_{(1-87)}$-Igκ-FAPα2-*STE2* (yAEA153), $Mfα1_{(1-83)}$-FAPα2-*STE2* (yAEA169), $Mfα1_{(1-83)}$-$Igκ_{(1-10)}$-FAPα2-*STE2* (hereafter "FAP-Ste2") (yAEA170), $Mfα1_{(1-87)}$-$Igκ_{(1-10)}$-FAPα2-*STE2* (yAEA171), $Ste2_{(1-51)}$-Igκ-FAPα2-*STE2* (yAEA172), $Ste2_{(1-51)}$-FAPα2-*STE2* (yAEA173), $Suc2_{(1-19)}$-Igκ-FAPα2-*STE2* (yAEA205), and $Suc2_{(1-19)}$-FAPα2-*STE2* (yAEA206), from the endogenous *STE2* promoter were grown to early-exponential phase, harvested, lysed, and the membrane fraction prepared, resolved by SDS-PAGE, and analyzed by immunoblotting. (C) *Left*, pheromone sensitivity of each strain listed in (B) was assessed using an agar diffusion (halo) bioassay for α-factor-induced growth arrest. Plates contained BSM medium and α-factor in aqueous solution was spotted on each filter (15 μg total per disk). A representative experiment is shown. *Right*, average halo diameters from two independent experiments each performed in triplicate are plotted as a bar graph. Error bars, standard error of the mean (SEM). (D) The strains listed in (B) were grown to early-exponential phase, incubated with fluorogen at 30˚C for 15 min and imaged by fluorescence microscopy and fluorescence intensities quantified using CellProfiler, as described in Materials and Methods. The data are plotted as box-and-whisker plots, in which each box represents the interquartile range (IQR) between the lower quartile (25%) and the upper quartile (75%), the horizontal black line indicates the median value, and the whisker ends represent the lowest and highest data point still within 1.5 IQR of the lower and upper quartile, respectively.

FIG. S3

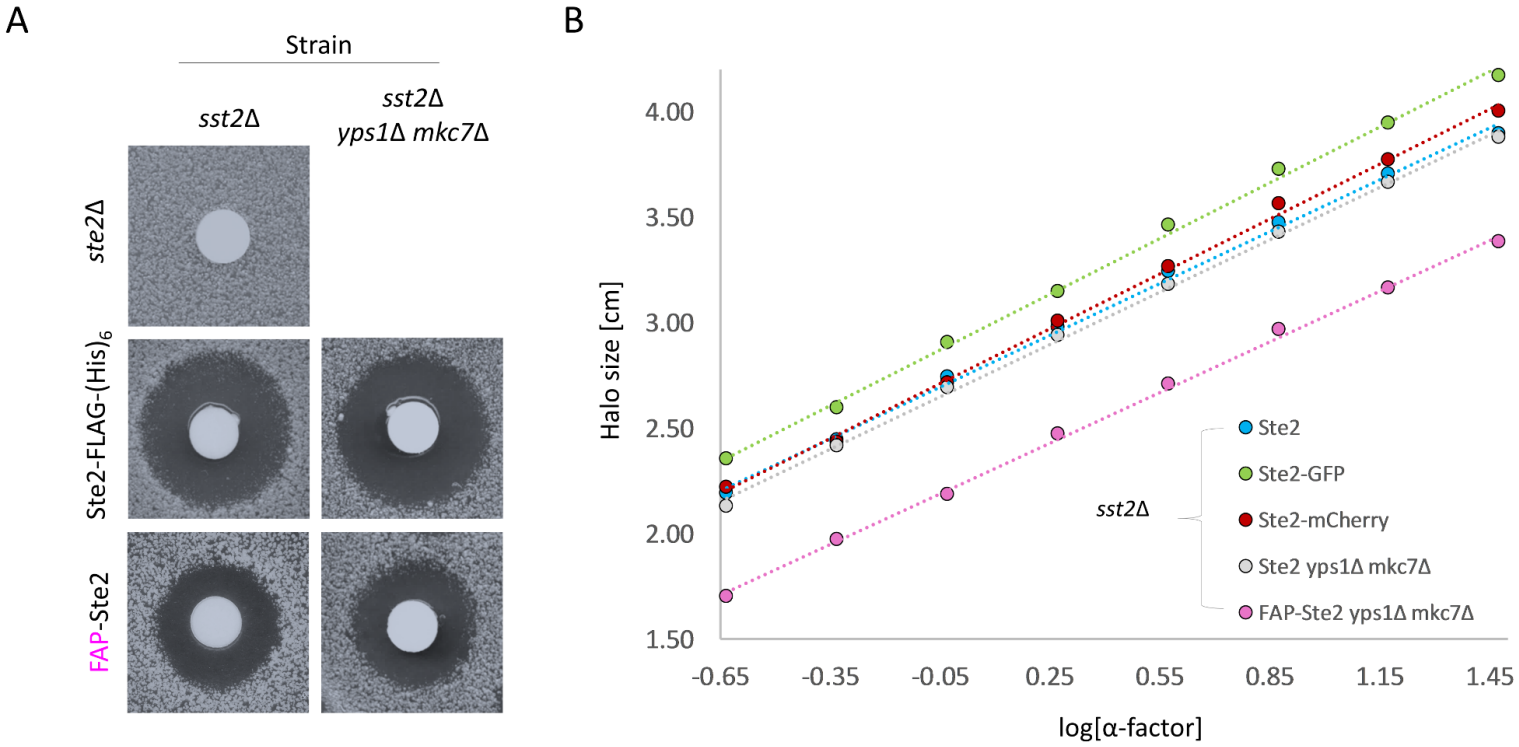

Fig. S3. Response of FAP-Ste2-expressing cells to α-factor. (A) Pheromone sensitivity of *MAT***a** *sst2*Δ cells lacking Ste2 (*ste2*Δ) (yDB103) (*top*), or otherwise isogenic derivatives also lacking yapsins (*yps1*Δ *mkc7*Δ) and expressing either Ste2-FLAG-$(His)_6$ (yAEA260 and yAEA372, respectively) *or* FAP-Ste2 (yAEA256 and yAEA373, respectively) from the endogenous *STE2* locus was determined as described in the legend to Fig. S2C, except that 0.25 μg of α-factor was applied to each filter disk. (B) The strains shown in (A), as well as *MAT***a** *sst2*Δ cells expressing Ste2-EGFP (yAEA257) or Ste2-mCherry (yAEA258), were analyzed as in (A) over a range of α-factor amounts (0.125 - 30 μg) and the average values of halo diameter from independent trails (n = 6) plotted against the amount of pheromone.

FIG. S4

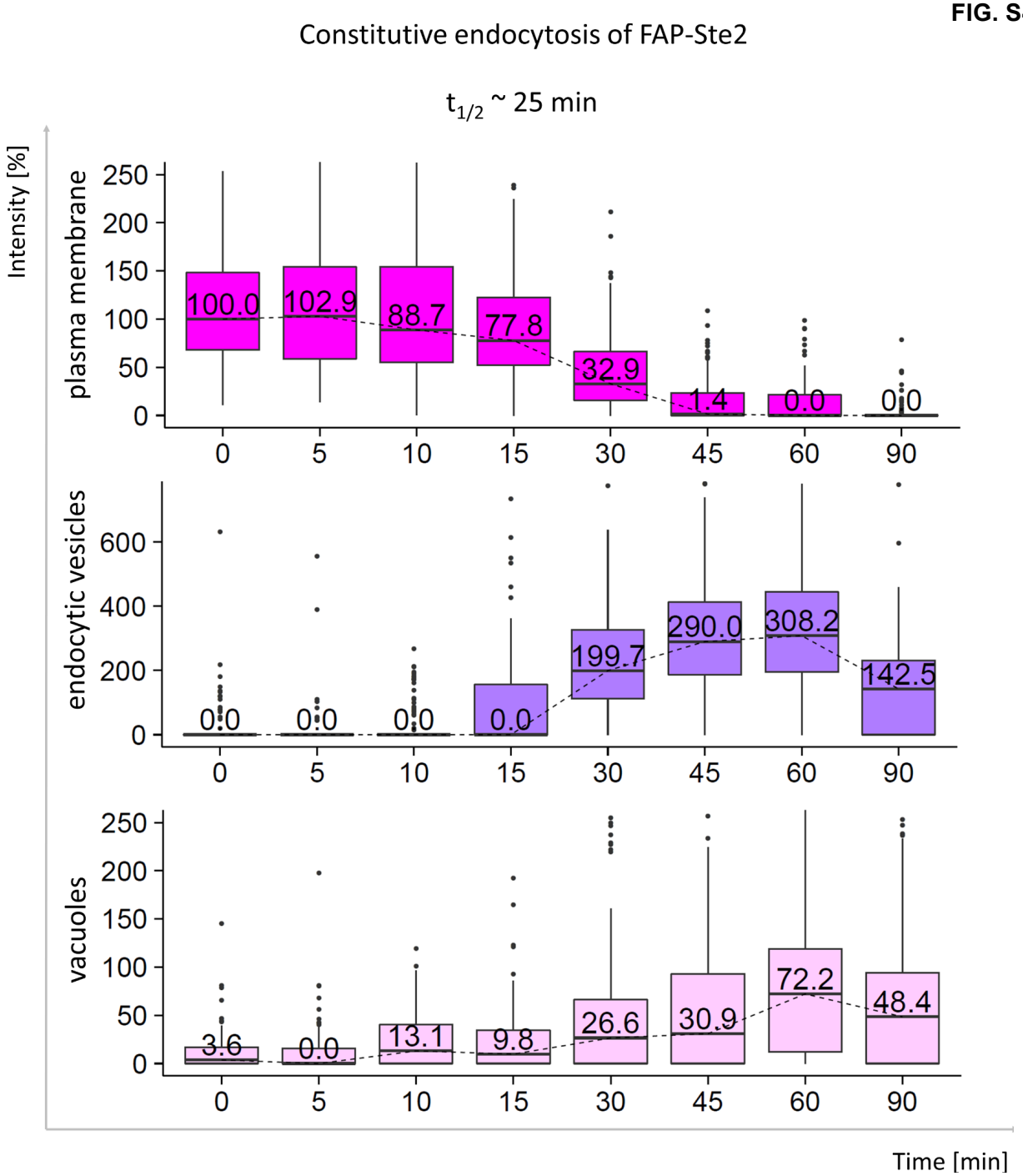

Fig. S4. FAP-Ste2 internalized by basal endocytosis is delivered to and degraded in the vacuole. Cultures of *MAT***a** FAP-Ste2 Vph1-EGFP *yps1*Δ *mkc7*Δ cells (yAEA380) were grown to early-exponential phase, incubated with LatA and fluorogen, mounted onto glass bottoms of imaging chambers, as described in detail in Materials and Methods. After LatA wash out (which also removes any excessive fluorogen), localization of FAP-Ste2 was monitored by fluorescence microscopy over the course of 90 min. The resulting fluorescent images were quantified using CellProfiler and plotted as in Fig. 6B. *Inset*, half-time for removal of FAP-Ste2 from the PM was ~25 min.

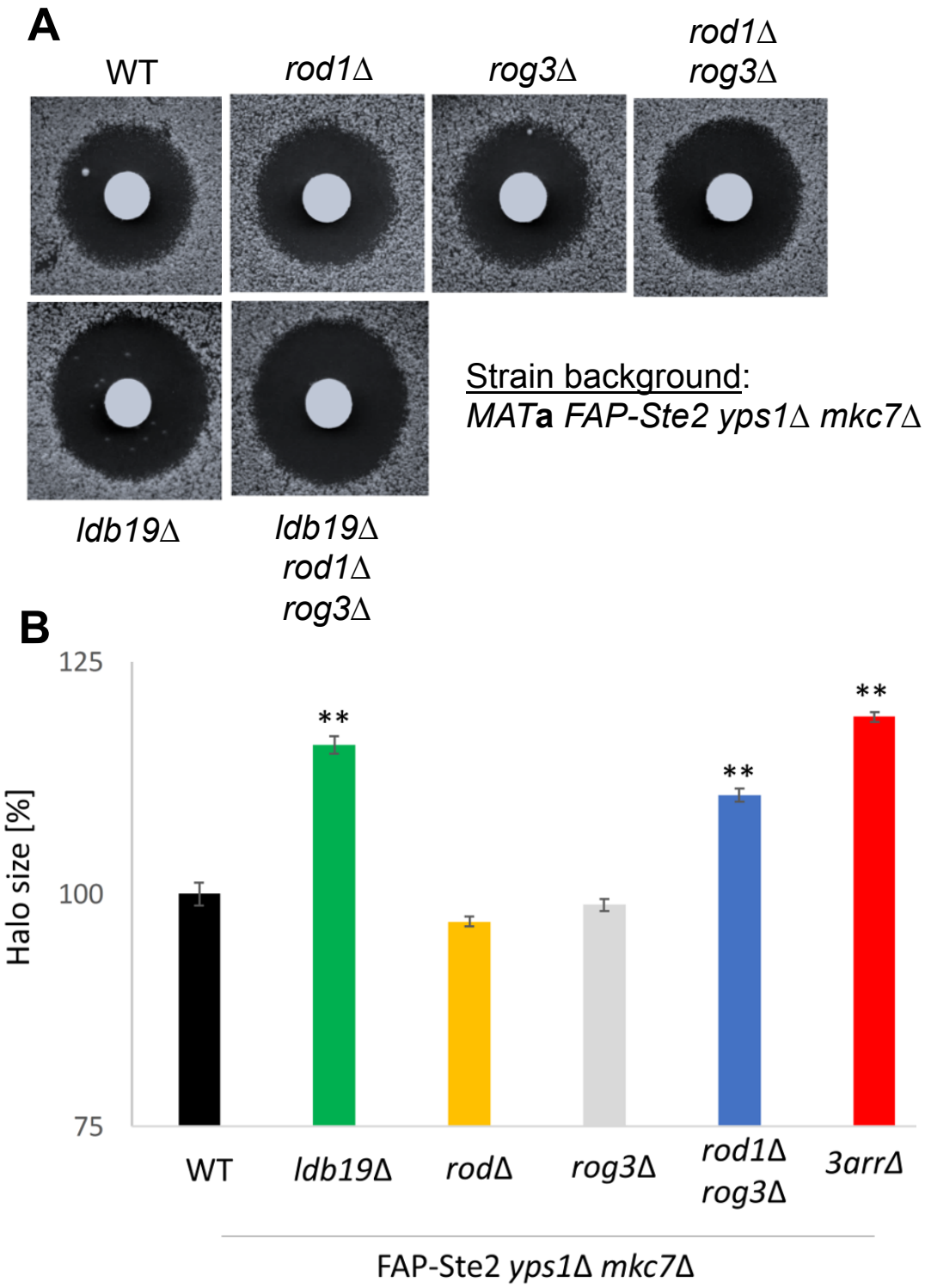

FIG. S5

Fig. S5. Removal of specific α-arrestins enhances in an additive manner the pheromone sensitivity of yapsin-deficient cells expressing FAP-Ste2. Otherwise isogenic derivatives of a *MAT***a** *yps1*Δ *mkc7*Δ FAP-*STE2* Vph1-EGFP strain ("WT") (yAEA380) lacking Rod1 (*rod1*Δ) (yAEA384), or Rog3 (*rog3*Δ) (yAEA385), or both Rod1 and Rog3 (*rod1*Δ *rog3*Δ) (yAEA388), or Ldb19 (ldb19Δ) (yAEA383), or all three α-arrestins (*3arrΔ*) (yAEA381), were tested for pheromone responsiveness as described in the legend to Fig. S2C. Representative data from a single experiment are shown. (B) Average halo diameters from two independent experiments each performed in triplicate are plotted as a bar graph. Error bars, standard error of the mean (SEM). Double asterisk (**), $p<0.0001$, determined by two-tailed Student's t-test.